arXiv:1403.5200v1 [cond-mat.mes-hall] 20 Mar 2014

Mechanically-controlled spin-selective transport

R. I. Shekhter,[1] O. Entin-Wohlman,[2,3] and A. Aharony[2,3]

[1]*Department of Physics, Göteborg University, SE-412 96 Göteborg, Sweden*
[2]*Raymond and Beverly Sackler School of Physics and Astronomy, Tel Aviv University, Tel Aviv 69978, Israel*
[3]*Physics Department, Ben Gurion University, Beer Sheva 84105, Israel*

(Dated: March 21, 2014)

A device enabling mechanically-controlled spin and electric transport in mesoscopic structures is proposed. It is based on the transfer of electrons through weak links formed by suspended nanowires, on which the charge carriers experience a strong Rashba spin-orbit interaction that twists their spins. It is demonstrated that when the weak link bridges two magnetically-polarised electrodes, a significant spintro-voltaic effect takes place. Then, by monitoring the generated voltage one is able to measure electronic spins accumulated in the electrodes, induced e.g., by circularly-polarised light, or alternatively, the amount of spin twisting. Mechanically-tuning the device by bending the nanowire allows one to achieve full control over the spin orientations of the charge carriers.

PACS numbers: 07.10Cm,72.25.Hg,72.25.Rb

I. INTRODUCTION

Achieving significant interplay among the electric, magnetic, and mechanical degrees of freedom in solid-state devices suggests exciting perspectives in coherent operations involving all three of them. Charge carriers in conducting materials are perfect candidates for realising such an interplay since they carry both electric charges and magnetic moments (their spins) and can be coupled quite strongly to mechanical deformations in beamlike mesoscopic setups.

Indeed, experiments have demonstrated[1–6] the feasibility of coupling charge carriers to mechanical vibrations of suspended nanodevices, showing, e.g., that a mechanically-vibrating single-walled carbon nanotube can also act concomitantly as a single-electron transistor. The role of the spin degree of freedom, i.e., the generation, detection and exploitation of spin currents, has been recently discussed quite extensively, in particular in conjunction with the spin Seebeck effect in the magnetic insulator yttrium-iron garnet.[7] This effect refers to the generation of an electric power from a temperature difference between the magnetic insulator and a layer of normal metal attached to it.[8–11] The temperature difference gives rise to a spin current which is pumped into the normal metal in a longitudinal configuration, and induces there a traverse emf via the inverse spin Hall effect.[12,13] The companion phenomenon, i.e., the spin Peltier effect, has been detected as well.[14] Thermally-activated spin current through ferromagnetic tunnel contacts has been detected in Ref. 15.

A particularly-promising situation arises when the electric current through a mechanically-deformed weak link is provided by a battery of uncompensated electronic spins. Such a setup combines together all three types of degrees of freedom and allows for a plethora of intriguing phenomena. When the magnetic polarisations in the electronic reservoirs forming the electrodes are not identical, then quite generally both charge and spin currents result from the transport of electrons through the junction. The situation at hand resembles in a way thermoelectric transport in a two-terminal junction: the two currents (charge and spin), flow in response to two affinities, the voltage difference and the difference in the amount of magnetic polarisation between the two reservoirs. "Non-diagonal" phenomena, analogous to the thermoelectric Seebeck and Peltier effects, can therefore be expected. For instance, it is possible to generate a spin current by injecting charges into the material, which in turn may give rise to a spatially inhomogeneous spin accumulation.

However, the two opposite spins can still contribute equally to the charge transport, resulting in zero net spin propagation, much like the vanishing of the thermopower when electron-hole symmetry is maintained. In the case of combined spin and charge transport, non-diagonal spin-electric effects appear once the spin and charge transports are coupled in a way that distinguishes between the two spin projections. One may achieve such a spin-dependent transport by exploiting magnetic materials in which the electronic energy is spin-split. When the magnetization is spatially inhomogeneous (as happens in composite magnetic structures) the spin-dependent part of the energy will be inhomogeneous as well, leading to a spin-dependent force acting on the charge carriers. Another possibility, feasible even in magnetically-homogeneous materials, is to employ the Rashba spin-orbit interaction[16] which can be controlled by external electric fields. This interaction causes the electronic spin to rotate around an axis determined by its spin and the electric-field direction.[17] When this interaction varies in space, the electronic spin is twisted. The end result is the same as in the first scenario above: a spin-dependent force (resulting from the Rashba interaction) is exerted on the electrons, opening the way for non-diagonal spintro-electric transport.

Obviously, making such a spintro-electric effect tunable and controllable would be of great importance both from the viewpoint of fundamental physics as well as from that of practical applications. Here we propose that such a manipulation of the spintro-electric transport can be

achieved by confining the spin-orbit interaction into a small domain in space, that at the same time can also be mechanically treated. In other words, one can modify geometrically the spatial region where the spin-orbit interaction takes place. When this very domain also serves as a weak link, both the spin-orbit coupling and the electric resistance can be controlled through a geometrical deformation of the device. Such an arrangement can be realized in electronic weak links or microconstrictions; it makes room for the possibility of controlling the transport by modifying the electronic scattering in a small region of the material around the junction. Specifically, we suggest that a suspended nanowire is most suitable for playing the role of the desired weak link. It is known that the Rashba spin-orbit interaction is anomalously large in certain nanowires[18] and also in nanotubes.[19] These beamlike structures are beneficial for our purposes since they are likely to produce spin twist due to the Rashba interaction, while mechanically controlling their bending allows for the manipulation of the amount of twisting. This possibility arises because mechanically bending carbon nanotubes directly modifies the ballistic motion of the electrons through them, via the spin torque exerted by the Rashba spin-orbit interaction.[20]

Below we present a complete description of the spintro-electric transport through a Rashba spin-twister and demonstrate the non-diagonal effects that are possible in such a device. Section II presents the general formulation for the transport of the spin and the charge through a vibrating weak link, in the presence of both an Aharonov-Bohm flux and a Rashba spin-orbit interaction. The results are summarised by the 3×3 linear-response matrix of transport coefficients, Eqs. (22) and (23). Explicit expressions for these coefficients are derived in Sec. III, and given in Eq. (30). Section III also considers several special cases, showing how one can generate a voltage without a charge current across an open circuit by a spin imbalance in the reservoirs (see Fig. 1), and how one can change the spin twisting by bending the weak link wire. Our conclusions are given in Sec. IV. Certain detailed calculations are relegated to Appendix A.

II. SPINTRO-VOLTAIC EFFECTS DUE TO RASHBA SPLITTING

A. General approach

A ubiquitous description of transport phenomena through electronic weak links is based on the assumption that the electric resistance of the weak link dominates the resistance of the entire device.[21] This assumption means that the distribution of the electrons in momentum space in each of the electronic reservoirs follows locally the equilibrium one. The electric current through the weak link is then accomplished by tunnel coupling. Here we adopt this approach. However, having the electronic spin as an active component in the transport, this scheme needs to be extended to include also the distribution of the electrons in spin space. The latter depends on the specific experimental setup. For instance, injecting spin-polarised electrons into each of the electrodes when the spin-relaxation rate there is slow enough yields "spin pumping",[22] which results in an imbalance between oppositely-oriented electronic spins. Under these circumstances the electrochemical potential that determines the local equilibrium distribution in each of the electrodes will be different for the two spin projections. A similar situation can be created upon using circularly-polarised light to pump excess spins into an electronic system.[23] More options are open when the electrodes are made of magnetic materials. In that case the spin polarisation of the electrons induced by the internal magnetization can differ from the one invoked by an external injection. The actual electronic distribution in spin space has then to be determined from an additional kinetic equation, a task which is beyond the scope of the present study. Instead, we will assume that the spin orientation of the injected electrons coincides with the direction of the internal magnetization in magnetic reservoirs.[24]

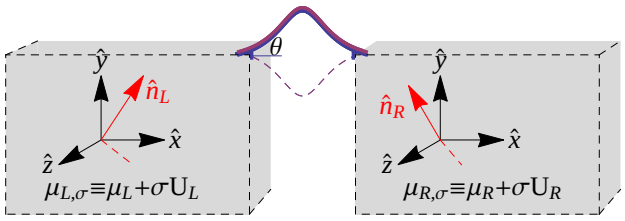

FIG. 1: A schematic representation of the proposed setup. A nanowire, bended in the $x-y$ plane is coupled to two magnetically-polarised electronic reservoirs with arbitrarily-oriented magnetization axes $\hat{\mathbf{n}}_L$ and $\hat{\mathbf{n}}_R$. The externally-pumped spins give rise to a spin-dependent electrochemical potentials $\mu_{L(R),\sigma} \equiv \mu_{L(R)} + \sigma U_{L(R)}$. The bending of the nanowire is specified by the angle it makes with the $\hat{\mathbf{x}}-$axis, with an instantaneous value θ around the equilibrium angle θ_0.

The setup we propose is depicted schematically in Fig. 1. It comprises of a nanowire bridging two leads, firmly coupled to the left and right electronic reservoirs, held at spin-dependent electrochemical potentials $\mu_{L,\sigma} \equiv \mu_L + \sigma U_L$ and $\mu_{R,\sigma} \equiv \mu_R + \sigma U_R$, respectively (the notations L and R refer to the left and the right leads, see Fig. 1). Here σ is the spin index. The two bulk metals forming the reservoirs are each polarised along its own polarisation axis, denoted by the unit vectors $\hat{\mathbf{n}}_L$ and $\hat{\mathbf{n}}_R$, respectively. The wire vibrates in the $x-y$ plane, such that the angle θ it makes with the $\hat{\mathbf{x}}-$axis oscillates around an equilibrium value, θ_0. An additional (weak)

magnetic field, applied along the $\hat{\mathbf{z}}-$direction, gives rise to an instantaneous Aharonov-Bohm effect,[25] modifying the transport properties of the device and thus adding to its versatility.

The spin-resolved current through such a Rashba spin-junction was considered in detail in Ref. 20. The model exploited in the explicit calculations replaces the nanowire by a quantum dot[26] that has a single level, of energy ϵ_0. As explained above, the reservoirs are represented by their respective electronic distributions determined by the spin-dependent electrochemical potentials,

$$f_{L,\sigma}(\epsilon_{k,\sigma}) = [e^{\beta(\epsilon_{k,\sigma}-\mu_{L,\sigma})}+1]^{-1} \ ,$$
$$f_{R,\sigma'}(\epsilon_{p,\sigma'}) = [e^{\beta(\epsilon_{p,\sigma'}-\mu_{R,\sigma'})}+1]^{-1} \ , \qquad (1)$$

with $\beta^{-1} = k_{\rm B}T$. The electron gas states in the left (right) reservoir are indexed by k,σ (p,σ') and have energies $\epsilon_{k,\sigma}$ $(\epsilon_{p,\sigma'})$.

The linear Rashba interaction manifests itself by phase factors multiplying the tunneling amplitudes that couple the nanowire to the leads.[27] In the geometry of Fig. 2, these phases are induced by an electric field perpendicular to the $x-y$ plane. The phase factors are given by $\exp[i\alpha\mathbf{R}\times\boldsymbol{\sigma}\cdot\hat{\mathbf{z}}]$, where α denotes the strength of the spin-orbit interaction (in units of inverse length; units in which $\hbar=1$ are used), and $\boldsymbol{\sigma}$ is the vector of the Pauli matrices. Quite generally $\mathbf{R}=\mathbf{R}_L\equiv\{x_L,y_L\}$ for the left tunnel coupling and $\mathbf{R}=\mathbf{R}_R\equiv\{x_R,-y_R\}$ for the right one, where both radius vectors $\mathbf{R}_L$ and $\mathbf{R}_R$ are functions of the vibrational degrees of freedom (see Fig 2). We adopt the plausible geometry $y_L=y_R=(d/2)\sin(\theta)$ and $x_L=x_R=(d/2)\cos(\theta)$, where d is the wire length (θ is the instantaneous bending angle).[28] In order to mimic the bending vibrations of the wire we assume that once the wire is bended by the (equilibrium) angle θ_0, then the distance along x between the two supporting leads is fixed, while the (red) dot in Fig. 2 vibrates along y. As a result, $\tan(\theta)=2y/[d\cos(\theta)]$, implying that $\Delta\theta=(2/[d\cos(\theta)])\cos^2(\theta_0)\Delta y$. [$d\cos(\theta_0)$ is the wire projection on the $x-$direction.] It follows that

$$\theta=\theta_0+\Delta\theta=\theta_0+[a_0\cos(\theta_0)/d](b+b^\dagger) \ , \qquad (2)$$

where a_0 is the amplitude of the zero-point oscillations, and b ($b^\dagger$) is the destruction (creation) operator of the vibrations. Their free Hamiltonian is described by the Einstein model, $\mathcal{H}_{\rm vib}=\omega b^\dagger b$.

The quantum vibrations of the wire, i.e. the dynamics of the bending angle, make the electronic motion effectively two-dimensional.[25] This leads to the possibility of further manipulating the device via the Aharonov-Bohm effect, by applying a magnetic field perpendicular to the junction plane (see Fig. 2). This field imposes an additional phase on the tunneling amplitudes $\phi_{L(R)}=-(\pi/\Phi_0)(Hx_{L(R)}y_{L(R)})$ for the left and the right sides, respectively, where H is the magnetic field (a factor of order unity[25] is absorbed in H). The transport through the Rashba junction depends only on the total Aharonov-Bohm phase, ϕ,

$$\phi\equiv\phi_L+\phi_R$$
$$=-\frac{\pi H}{\Phi_0}(x_Ly_L+x_Ry_R)=-\frac{\pi Hd^2}{4\Phi_0}\sin(2\theta) \ , \qquad (3)$$

measured in units of the flux quantum $\Phi_0=hc/e$.

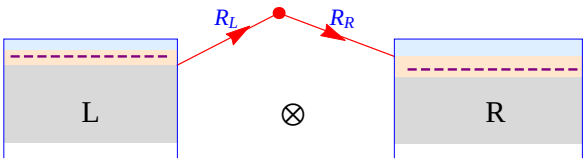

FIG. 2: Schematic geometry used for calculating the spin-orbit coupling dependence of the effective tunneling amplitude. A localized level is tunnel-coupled to left (L) and right (R) electronic electrodes. The setup lies in the $x-y$ plane; a magnetic field applied along $\hat{\mathbf{z}}$ is shown by $\otimes$. The radius vectors $\mathbf{R}_L$ and $\mathbf{R}_R$ connect the quantum dot with the left and right electrodes.

The end result of the above considerations is that the tunneling through the Rashba weak link is effectively described by a tunneling Hamiltonian connecting directly the left and the right electrodes,[20]

$$\mathcal{H}^{\rm e}_{\rm tun}=\sum_{k,p}\sum_{\sigma,\sigma'}(c^\dagger_{p,\sigma'}[W_{pk}]_{\sigma'\sigma}c_{k,\sigma}+{\rm H.c.}) \ , \qquad (4)$$

where $c_{k,\sigma}$ and $c^\dagger_{k,\sigma}$ ($c_{p,\sigma'}$ and $c^\dagger_{p,\sigma'}$) are the annihilation and creation operators of the electrons in the left (right) electrode. To second order in the (original) tunnelling amplitudes, the effective tunneling is[20]

$$[W_{pk}]_{\sigma'\sigma}=\frac{1}{2}\sum_{\widetilde{\sigma}}V_{p,\sigma'\widetilde{\sigma}}V_{k,\widetilde{\sigma}\sigma}\Big(\frac{1}{\epsilon_{k,\sigma}-\epsilon_0}+\frac{1}{\epsilon_{p,\sigma'}-\epsilon_0}\Big) \ . \qquad (5)$$

The tunneling amplitudes between the left and the right electrodes and the quantum dot, V_p and V_k respectively, (matrices in spinor space) consist of the "bare" tunneling amplitudes (denoted J_L and J_R, respectively), and the phases describing the effects of the perpendicular (Aharonov-Bohm) magnetic field and the Rashba interaction,

$$V_{k(p)}=-J_{L(R)}\exp[-i\psi_{L(R)}] \ , \qquad (6)$$

where

$$\psi_L=\phi_L-\alpha(x_L\sigma_y-y_L\sigma_x) \ ,$$
$$\psi_R=\phi_R-\alpha(x_R\sigma_y+y_R\sigma_x) \ . \qquad (7)$$

The spin-resolved particle current emerging from the left electrode, $I_{L,\sigma}$, is found[20] by calculating the time evolution of the number operator of electrons with spin projection σ, $\dot{N}_{L,\sigma}$,

$$-I_{L,\sigma} \equiv \dot{N}_{L,\sigma} = \int_0^\infty d\tau \sum_{k,p,\sigma'} \Big[f_{R,\sigma'}(\epsilon_{p,\sigma'})[1-f_{L,\sigma}(\epsilon_{k,\sigma})] \tag{8}$$
$$\times \Big(e^{i(\epsilon_{k,\sigma}-\epsilon_{p,\sigma'})\tau} \langle [W_{pk}]_{\sigma'\sigma} [W^\dagger_{kp}(\tau)]_{\sigma\sigma'} \rangle + e^{i(\epsilon_{p,\sigma'}-\epsilon_{k,\sigma})\tau} \langle [W_{pk}(\tau)]_{\sigma'\sigma} [W^\dagger_{kp}]_{\sigma\sigma'} \rangle \Big)$$
$$- f_{L,\sigma}(\epsilon_{k,\sigma})[1-f_{R,\sigma'}(\epsilon_{p,\sigma'})] \Big(e^{i(\epsilon_{p,\sigma'}-\epsilon_{k,\sigma})\tau} \langle [W^\dagger_{kp}]_{\sigma\sigma'} [W_{pk}(\tau)]_{\sigma'\sigma} \rangle + e^{i(\epsilon_{k,\sigma}-\epsilon_{p,\sigma'})\tau} \langle [W^\dagger_{kp}(\tau)]_{\sigma\sigma'} [W_{pk}]_{\sigma'\sigma} \rangle \Big) \Big] \ .$$

An analogous expression gives the current emerging from the right electrode. The angular brackets in Eq. (8) denote thermal averaging over the vibrations and over their time evolution with respect to the Einstein Hamiltonian. Assuming off-resonance conditions, the wave vector-dependence of the effective tunneling amplitude may be discarded, and then [see Eq. (5)]

$$\langle [W_{pk}]_{\sigma'\sigma} [W^\dagger_{kp}(\tau)]_{\sigma\sigma'} \rangle = \frac{J_L^2 J_R^2}{\epsilon_0^2}$$
$$\times \langle [e^{-i\psi_R} e^{-i\psi_L}]_{\sigma'\sigma} [e^{i\psi^\dagger_L(\tau)} e^{i\psi^\dagger_R(\tau)}]_{\sigma\sigma'} \rangle \ , \tag{9}$$

[note that $\psi_{L,R} = \psi^\dagger_{L,R}$, see Eqs. (7)] with

$$\langle [e^{-i\psi_R} e^{-i\psi_L}]_{\sigma'\sigma} [e^{i\psi^\dagger_L(\tau)} e^{i\psi^\dagger_R(\tau)}]_{\sigma\sigma'} \rangle$$
$$= \sum_{n,n'} P(n) e^{i(n'-n)\omega\tau} |\langle n| [e^{-i\psi_R} e^{-i\psi_L}]_{\sigma'\sigma} |n'\rangle|^2 \ . \tag{10}$$

Here $|n\rangle$ and $|n'\rangle$ denote the eigenstates of energies $(n+1/2)\omega$ and $(n'+1/2)\omega$, respectively, of the Einstein vibrations, and

$$P(n) = \frac{e^{-(n+1/2)\beta\omega}}{\mathrm{Tr} e^{-\beta \mathcal{H}_{\rm vib}}} = e^{-n\beta\omega}(1-e^{-\beta\omega}) \ , \tag{11}$$

such that $\sum_{n=0}^\infty P(n) = 1$ and $\sum_{n=0}^\infty P(n) n = 1/[e^{\beta\omega}-1] \equiv N_B(\omega)$ is the Bose-Einstein distribution. The other thermal averages in Eq. (8) are expressed in a similar form.

Since the electrodes are magnetically-polarised, the density of states in each of them depends on both the internal exchange interaction and the external spin pumping as expressed by the energy split of the electrochemical potentials $U_{L,R}$ that determine the kinetic energy of the electrons participating in the transport. However, the latter dependence is weak and to lowest order in $U_{L,R}/\mu$, where $\mu = (\mu_L + \mu_R)/2$ is the common chemical potential of the entire device, it may be neglected. Therefore, upon converting the sums over the wave vectors in Eq. (8) into integrals it turns out that the spin-resolved particle currents emerging from the left and the right electrodes are

$$-I_{L,\sigma} = 2\pi \mathcal{N}_{L,\sigma} \sum_{\sigma'} \mathcal{N}_{R,\sigma'} \sum_{n,n'=0}^\infty P(n) \mathcal{T}_{nn',\sigma\sigma'}$$
$$\times (1 - e^{\beta(\mu_{L,\sigma}-\mu_{R,\sigma'})}) \frac{\mu_{L,\sigma} - \mu_{R,\sigma'} + (n'-n)\omega}{e^{\beta[\mu_{L,\sigma}-\mu_{R,\sigma'}+(n'-n)\omega]}-1} \ , \tag{12}$$

and

$$-I_{R,\sigma'} = 2\pi \mathcal{N}_{R,\sigma'} \sum_{\sigma} \mathcal{N}_{L,\sigma} \sum_{n,n'=0}^\infty P(n) \mathcal{T}_{nn',\sigma\sigma'}$$
$$\times (e^{\beta(\mu_{L,\sigma}-\mu_{R,\sigma'})} - 1) \frac{\mu_{L,\sigma} - \mu_{R,\sigma'} + (n'-n)\omega}{e^{\beta[\mu_{L,\sigma}-\mu_{R,\sigma'}+(n'-n)\omega]}-1} \ . \tag{13}$$

Clearly particle number is conserved, as can be seen by adding together Eq. (12) summed over σ and Eq. (13) summed over σ'.

The spin indices of the matrix element squared[29] forming the transmission, $\mathcal{T}$, in Eqs. (12) and (13) deserve some caution: the quantization axes of the magnetization in the two electronic reservoirs are generally different (see Fig. 1), and they both may differ from the quantization axis which is used to describe the Rashba interaction on the nanowire. Specifying the quantization axis in the left (right) reservoir by the angles θ_L (θ_R) and φ_L (φ_R), then

$$\mathcal{T}_{nn',\sigma\sigma'} = \Big(\frac{J_L J_R}{\epsilon_0} \Big)^2 |\langle n| [\mathcal{S}^\dagger_R e^{-i\psi_R} e^{-i\psi_L} \mathcal{S}_L]_{\sigma'\sigma} |n'\rangle|^2 \ , \tag{14}$$

where the rotation transformations $\mathcal{S}_{L(R)}$ are given by

$$\mathcal{S}_{L(R)} = \begin{bmatrix} e^{-i\frac{\varphi_{L(R)}}{2}} \cos\frac{\theta_{L(R)}}{2} & e^{-i\frac{\varphi_{L(R)}}{2}} \sin\frac{\theta_{L(R)}}{2} \\ e^{i\frac{\varphi_{L(R)}}{2}} \sin\frac{\theta_{L(R)}}{2}) & -e^{i\frac{\varphi_{L(R)}}{2}} \cos\frac{\theta_{L(R)}}{2} \end{bmatrix} \ . \tag{15}$$

For instance, when the quantization axes in both electrodes are identical, $\hat{\mathbf{n}}_L = \hat{\mathbf{n}}_R$, then $\mathcal{S}$ just rotates the direction of the quantization axis of the Rashba interaction.

B. The linear-response regime

As is mentioned above, the transport of the charge carriers in our setup consists of both charge and spin currents. Here we examine these currents in the linear-response regime, where the spin-resolved particle currents, Eqs. (12) and (13) become

$$I_{L,\sigma} = 2\pi \mathcal{N}_{L,\sigma} \sum_{\sigma'} \mathcal{N}_{R,\sigma'} (\mu_{L,\sigma} - \mu_{R,\sigma'}) \mathcal{A}_{\sigma\sigma'} \ ,$$
$$I_{R,\sigma'} = 2\pi \mathcal{N}_{R,\sigma'} \sum_{\sigma} \mathcal{N}_{L,\sigma} (\mu_{R,\sigma'} - \mu_{L,\sigma}) \mathcal{A}_{\sigma\sigma'} \ , \tag{16}$$

with the transmission

$$\mathcal{A}_{\sigma\sigma'} = \sum_{n=0}^{\infty} P(n)\mathcal{T}_{nn,\sigma\sigma'} + \sum_{\substack{nn'=0 \\ n\neq n'}}^{\infty} P(n)\mathcal{T}_{nn',\sigma\sigma'} \frac{(n'-n)\beta\omega}{e^{(n'-n)\beta\omega}-1} \ . \quad (17)$$

The first term in Eq. (17) gives the contribution to the spin-resolved transport from the elastic tunneling processes. The second is due to the inelastic processes, and is active at finite temperatures.

Our final expressions for the charge currents are then

$$eI_L \equiv e\sum_\sigma I_{L,\sigma} = e(\mu_L-\mu_R)\mathcal{C}_1 - eU_R\mathcal{C}_3 + eU_L\mathcal{C}_2 \ , \quad (18)$$

with $eI_R \equiv e\sum_{\sigma'} I_{R,\sigma'} = -eI_L$. The spin currents emerging from the left and right reservoirs are

$$I_L^{\rm spin} \equiv \sum_\sigma \sigma I_{L,\sigma} = (\mu_L-\mu_R)\mathcal{C}_2 - U_R\mathcal{C}_4 + U_L\mathcal{C}_1 \ ,$$
$$I_R^{\rm spin} = \sum_{\sigma'} \sigma' I_{R,\sigma'} = (\mu_R-\mu_L)\mathcal{C}_3 + U_R\mathcal{C}_1 - U_L\mathcal{C}_4 \ . \quad (19)$$

In Eqs. (18) and (19) we have introduced the linear-response transport coefficients

$$\mathcal{C}_1 = 2\pi\sum_{\sigma\sigma'} \mathcal{N}_{L,\sigma}\mathcal{A}_{\sigma\sigma'}\mathcal{N}_{R,\sigma'} \ ,$$
$$\mathcal{C}_2 = 2\pi\sum_{\sigma\sigma'} \mathcal{N}_{L,\sigma}\sigma\mathcal{A}_{\sigma\sigma'}\mathcal{N}_{R,\sigma'} \ ,$$
$$\mathcal{C}_3 = 2\pi\sum_{\sigma\sigma'} \mathcal{N}_{L,\sigma}\mathcal{A}_{\sigma\sigma'}\sigma'\mathcal{N}_{R,\sigma'} \ ,$$
$$\mathcal{C}_4 = 2\pi\sum_{\sigma\sigma'} \mathcal{N}_{L,\sigma}\sigma\mathcal{A}_{\sigma\sigma'}\sigma'\mathcal{N}_{R,\sigma'} \ , \quad (20)$$

giving the various transmission probabilities of the junction.[29]

C. The Onsager relations

As was mentioned in Sec. I, there is a certain analogy between the configuration studied here and that of thermoelectric transport. In order to further pursue this point we consider the entropy production in our device, assuming that the spin imbalance in each of the two reservoirs does not vary with time and that all parts of the setup are held at the same temperature T. Under these circumstances the entropy production, $\dot{S}$, is

$$T\dot{S} = \sum_\sigma \mu_{L,\sigma} I_{L,\sigma} + \sum_{\sigma'} \mu_{R,\sigma'} I_{R,\sigma'} = I_L(\mu_L-\mu_R) + U_L I_L^{\rm spin} + U_R I_R^{\rm spin} \ , \quad (21)$$

where the various currents are given in Eqs. (18) and (19). Obviously, the first term on the right-hand side of Eq. (21) is the dissipation due to Joule heating. The other two terms describe the dissipation involved with the spin currents.

As is seen from Eq. (21), the entropy production may be presented as a scalar product of the vector of driving forces (sometimes called "affinities"), $\{V \equiv (\mu_L-\mu_R)/e, U_L, U_R\}$ and the resulting currents, $\{eI_L, I_L^{\rm spin}, I_R^{\rm spin}\}$. In the linear-response regime (see Sec. II B) these two vectors are related to one another by a (3×3) matrix $\mathcal{M}$, which contains the transport coefficients,

$$\begin{bmatrix} eI_L \\ I_L^{\rm spin} \\ I_R^{\rm spin} \end{bmatrix} = \mathcal{M} \begin{bmatrix} V \\ U_L \\ U_R \end{bmatrix} \quad (22)$$

with

$$\mathcal{M} = \begin{bmatrix} e^2\mathcal{C}_1 & e\mathcal{C}_2 & -e\mathcal{C}_3 \\ e\mathcal{C}_2 & \mathcal{C}_1 & -\mathcal{C}_4 \\ -e\mathcal{C}_3 & -\mathcal{C}_4 & \mathcal{C}_1 \end{bmatrix} \ . \quad (23)$$

One notes that this matrix obeys the Onsager relations: reversing the sign of the magnetic field, i.e., inverting the sign of the Aharonov-Bohm phase ϕ [Eq. (3)] and concomitantly interchanging the vibration states indices n with n' and the spin indices σ with σ' in Eqs. (14) and (17) leaves all off diagonal terms in the matrix $\mathcal{M}$ unchanged.

III. SPIN-ELECTRIC TRANSPORT THROUGH A RASHBA TWISTER DEVICE

A. The transport coefficients

The full calculation of the transmission matrix $\mathcal{A}$ that determines the transport coefficients $\mathcal{C}_i$ [see Eqs. (17) and (20)] is quite complicated, and requires a numerical computation. We provide in Appendix A an approximate form for it, valid when the coupling of the charge carriers to the vibrational modes of the wire is weak. The approximation is based on the different magnitudes that coupling takes in the magnetic Aharonov-Bohm phase and in the Rashba one. In order to see this, it is expedient to present the phase factors in the transmission amplitude in the form

$$\exp(-i\psi_R)\exp(-i\psi_L) \equiv e^{-i\phi}(A + i\mathbf{B}\cdot\boldsymbol{\sigma}) \ , \quad (24)$$

[see Eqs. (6), (7), and (9)]. Here A and $\mathbf{B}$ are functions of the instantaneous bending angle θ, Eq. (2),

$$A = 1 - 2\cos^2(\theta)\sin^2(\alpha d/2) \ ,$$
$$\mathbf{B} = \{0, \cos(\theta)\sin(\alpha d), -\sin(2\theta)\sin^2(\alpha d/2)\} \ ,$$
$$A^2 + \mathbf{B}\cdot\mathbf{B} = 1 \ , \quad (25)$$

and ϕ is the instantaneous Aharonov-Bohm flux in dimensionless units, Eq. (3). The components of the spin-orbit vector $\mathbf{B}$ are given in the coordinate axes depicted in Fig. 1.

As can be observed from Eqs. (2), (6), and (7), the effect of the electron-vibration interaction on the Rashba coupling is of the order of the zero-point amplitude of the vibrations divided by the wire length, a_0/d. On the other hand, upon inserting Eq. (2) into Eq. (3) one finds that the Aharonov-Bohm phase is

$$\phi \simeq -\frac{\pi H d^2}{4\Phi_0}\sin(2\theta_0) - \frac{\pi a_0 d H}{2\Phi_0}\cos(\theta_0)\cos(2\theta_0)(b+b^\dagger)\ . \tag{26}$$

The dynamics of the Aharonov-Bohm flux is thus determined by the flux enclosed in an area of order $a_0 d$ divided by the flux quantum (see Appendix A). The latter ratio can be significantly larger than a_0/d. For instance, the length of a single-walled carbon nanotube is about $d = 1\mu$, while the vibrations' zero-point amplitude is estimated to be $10^{-5}\mu$. This leads to $a_0/d \simeq 10^{-5}$, while $(Ha_0 d)/\Phi_0$ is of the order of 10^{-2} for magnetic fields of the order of a few Teslas (at which the effect of the magnetic field on the transport through the Rashba weak link becomes visible).

The disparity between the way the electron-vibration coupling affects the Rashba phase factor and the manner by which it dominates the magnetic one results in a convenient (approximate) form for the transmission matrix $\mathcal{A}$.[29] We show in Appendix A that

$$\mathcal{A} = g(T,H)\left[\begin{array}{cc}\mathcal{A}_{\rm d} & \mathcal{A}_{\rm nd}\\ \mathcal{A}_{\rm nd} & \mathcal{A}_{\rm d}\end{array}\right]\ . \tag{27}$$

Here g is the transmission of the junction in the absence of the Rashba interaction; it depends on the temperature and on the perpendicular magnetic field,

$$g(T,H) = \Big(\frac{J_L J_R}{\epsilon_0}\Big)^2\Big(\sum_{n=0}^{\infty}P(n)|\langle n|e^{-i\phi}|n\rangle|^2 + \sum_{n=0}^{\infty}\sum_{\ell=1}^{\infty}P(n)|\langle n|e^{i\phi}|n+\ell\rangle|^2\frac{2\ell\beta\omega}{e^{\ell\beta\omega}-1}\Big)\ . \tag{28}$$

This quantity is discussed extensively in Ref. 25 where one may find its detailed dependence on the temperature and on the magnetic field. The spin-dependent part of the transmission is given by the matrix in Eq. (27),

$$\begin{aligned}&\mathcal{A}_{\rm d}+\mathcal{A}_{\rm nd} = 1\ ,\\ &\mathcal{A}_{\rm d}-\mathcal{A}_{\rm nd} = (A_0^2-B_0^2)\hat{\mathbf{n}}_L\cdot\hat{\mathbf{n}}_R + 2A_0\mathbf{B}_0\cdot\hat{\mathbf{n}}_L\times\hat{\mathbf{n}}_R\\ &\qquad\qquad + 2(\mathbf{B}_0\cdot\hat{\mathbf{n}}_L)(\mathbf{B}_0\cdot\hat{\mathbf{n}}_R)\ .\end{aligned} \tag{29}$$

Here A_0 and $\mathbf{B}_0$ are given by the values of A and $\mathbf{B}$ defined in Eqs. (25) at equilibrium, i.e., when the angle θ there is replaced by θ_0. Their physical meaning is explained in Sec. III B: $\mathcal{A}_{\rm nd} = \sin^2(\gamma)$, where γ is the twisting angle of the charge carriers' spins, and $\mathcal{A}_{\rm d} = \cos^2(\gamma)$.

Using the explicit expression (27) for the transmission matrix $\mathcal{A}$ it is straightforward to find the transport coefficients $\mathcal{C}_i$. Retaining only terms linear in the difference between the densities of states of the spin orientations, we obtain

$$\begin{aligned}&\mathcal{C}_1+\mathcal{C}_4 \simeq 8\pi g(T,H)\mathcal{A}_{\rm d}\mathcal{N}_L\mathcal{N}_R \simeq \mathcal{C}_2+\mathcal{C}_3\ ,\\ &\mathcal{C}_1-\mathcal{C}_4 \simeq 8\pi g(T,H)\mathcal{A}_{\rm nd}\mathcal{N}_L\mathcal{N}_R\ ,\\ &\mathcal{C}_2-\mathcal{C}_3 = 4\pi g(T,H)\mathcal{A}_{\rm nd}(\mathcal{N}_{L,\uparrow}\mathcal{N}_{R,\downarrow}-\mathcal{N}_{,\downarrow}\mathcal{N}_{R,\uparrow})\ ,\end{aligned} \tag{30}$$

where $\mathcal{N}_{L,R}$ is the total density of states of each electronic reservoir (summed over the two spin directions). Glancing at Eq. (18) for the charge current and taking into account the first of Eqs. (29), shows that the conductance, G, of the junction is independent of the spin-orbit interaction, and is given by[30]

$$G = 4\pi e^2\mathcal{N}_L\mathcal{N}_R g(T,H)\ . \tag{31}$$

Specific spintro-voltaic effects are considered below.

B. Rashba twisting

When the junction is not subject to a perpendicular magnetic field and the charge carriers passing through it do not collect an Aharonov-Bohm phase due to it, one may safely ignore the effect of the quantum flexural nano-vibrations of the suspended wire. Indeed, the electron-vibration coupling on the weak link is of order $a_0/d \simeq 10^{-5}$ for carbon nanotubes (see the model description in Secs. II A and III A, and Appendix A). This interaction is therefore not expected to modify significantly the transmission through the wire.

The scattering of the electrons' momentum, caused by the spatial constraint of their orbital motion inside the nanowire, also induces scattering of the electronic spins. The latter results from the spin-orbit Rashba interaction located at the wire. Consequently, an electronic wave having a definite spin projection on the magnetization vector of the lead from which it emerges, is not a spin eigen state in the other lead.

Thus, a pure spin state $|\sigma\rangle$ in one lead becomes a mixed spin state in the other,

$$|\sigma\rangle \Rightarrow \alpha_1|\sigma\rangle + \alpha_2|\overline{\sigma}\rangle\ , \tag{32}$$

with probability amplitude α_1 to remain in the original state, and probability amplitude α_2 for a spin flip ($\overline{\sigma} = -\sigma$). During the propagation through the weak link the spins of the charge carriers are twisted, as is described by the transmission amplitude [see Eqs. (24) and (A1)], $A_0 + i\mathbf{B}_0\cdot\boldsymbol{\sigma}$. It follows that the probability amplitude for a spin flip, α_2, is given by

$$\alpha_2 = [\mathcal{S}_R^\dagger(A_0 + i\mathbf{B}_0\cdot\boldsymbol{\sigma})\mathcal{S}_L]_{\sigma\overline{\sigma}}\ , \tag{33}$$

with $\mathcal{S}_{L,R}$ given in Eq. (15). The Rashba twisting angle, γ, can now be defined by

$$|\alpha_2| = \sin(\gamma)\ , \tag{34}$$

with

$$|\alpha_2|^2 = \sin^2(\gamma) = \mathcal{A}_{\rm nd} \ , \tag{35}$$

yielding a clear physical meaning to the transmissions $\mathcal{A}_{\rm d}$ and $\mathcal{A}_{\rm nd}$ [see Eqs. (29)]. For example, in the simplest configuration of parallel magnetizations in both electrodes, i.e.,

$$\hat{\mathbf{n}}_L = \hat{\mathbf{n}}_R \equiv \hat{\mathbf{n}} \ , \tag{36}$$

Eqs. (29) yield

$$\sin(\gamma) = [B_0^2 - (\hat{\mathbf{n}} \cdot \mathbf{B}_0)^2]^{1/2} \ . \tag{37}$$

Interestingly enough, in this simple configuration $\sin(\gamma)$ is determined by the component of the Rashba vector $\mathbf{B}_0$ normal to the quantization axis of the magnetization in the electrodes. Mechanically manipulating the bending angle that determines the direction of the Rashba vector $\mathbf{B}_0$, one may control the twisting angle γ. Note also that had the vectors $\hat{\mathbf{n}}_L$ and $\hat{\mathbf{n}}_R$ been antiparallel to one another then $\sin(\gamma) = [1 - B_0^2 + (\hat{\mathbf{n}} \cdot \mathbf{B}_0)^2]^{1/2}$.

An even more convenient way to monitor the twisting effect may be realized by studying the spintro-voltaic effect in an open circuit, i.e., when the total charge current vanishes. One then finds that the spin-imbalanced populations in the electrodes give rise to an electric voltage, V_{sv}. Assuming that the spin imbalances in the two reservoirs are identical, i.e., $U_L = U_R \equiv U$, Eq. (18) yields

$$V_{sv} = \frac{\mathcal{C}_3 - \mathcal{C}_2}{\mathcal{C}_1} U \ . \tag{38}$$

The ratio of the voltage created by the spin imbalance, V_{sv}, to the amount of spin imbalance in the electrodes (expressed by U) can be found upon using Eqs. (30), in conjunction with Eqs. (29) and (35),

$$V_{\rm sv} = \sin^2(\gamma) \frac{\mathcal{N}_{L\uparrow}\mathcal{N}_{R\downarrow} - \mathcal{N}_{L\downarrow}\mathcal{N}_{R\uparrow}}{\mathcal{N}_L \mathcal{N}_R} U \ . \tag{39}$$

The voltage generated by the Rashba interaction gives directly the twisting angle; the proportionality between $V_{\rm sv}/U$ and $\sin^2(\gamma)$ being the magnetic mismatch parameter of the junction.

IV. CONCLUSIONS

In this paper we have shown that one can have additional spintro-electric functionalities if one uses a vibrating suspended weak link, with both a magnetic flux and an (electric field dependent) Rashba spin-orbit interaction. The twisting of the electronic spins as they move between the (spin polarized) electrodes can be manipulated by the bias voltage, the bending of the weak link wire and the polarisations of the spins in the electrodes.

The traditional picture of twisting of the electronic spin is viewed quantum-mechanically as a splitting of the electronic wave in spin space. We have shown that the twisting angle, which determines the probability amplitude of such a splitting can be measured electrically through a spintro-voltaic effect. The Rashba device proposed in this paper is therefore a promising component to be incorporated into mesoscopic electronic circuits where quantum coherence determines various interference effects of electronic waves, splitted in both momentum - and spin spaces.

Acknowledgments

This work was supported by the Israeli Science Foundation (ISF) and the US-Israel Binational Science Foundation (BSF). Financial support from Swedish VR is greatly acknowledged. RIS acknowledges the hospitality of Ben Gurion University and the support of the Distinguished Scientist Visitor Program.

Appendix A: The transmission matrix

Here we detail the approximate calculation of the transmission probability $\mathcal{A}$, Eq. (17), confining ourselves to the case of weak coupling of the electrons to the vibrational modes.

We begin by re-writing the transmission $\mathcal{T}$, Eq. (14), in the form

$$\mathcal{T}_{nn'\sigma\sigma'} = \Big(\frac{J_L J_R}{\epsilon_0}\Big)^2 |\langle n| e^{-i(\phi_0 + \Delta\phi)} \times \Big[\mathcal{S}_R^\dagger [A_0 + \Delta A + i(\mathbf{B}_0 + \Delta\mathbf{B}) \cdot \boldsymbol{\sigma}] \mathcal{S}_L\Big]_{\sigma'\sigma} |n'\rangle|^2 \ . \tag{A1}$$

Here we have used Eqs. (24) and (25), expressing ϕ, A, and $\mathbf{B}$ as the sums of their equilibrium values, ϕ_0, A_0, and $\mathbf{B}_0$ [i.e., with θ in Eqs. (3) and (25) replaced by θ_0] and their dynamical parts that include the vibrations' operators and are denoted by $\Delta\phi$, ΔA, and $\Delta\mathbf{B}$. It is straightforward to verify that the terms including $\Delta A + i\Delta\mathbf{B}\cdot\boldsymbol{\sigma}$ contribute only when the electron-vibration interaction is accounted for at least to second order. In view of the smallness of the effect that interaction has on the Rashba coupling, as opposed to its effect on the magnetic phase (see the discussion in Sec. III A) we omit those terms, keeping the electron-vibration interaction only in the magnetic phase. As a result we obtain

$$\mathcal{T}_{nn'\sigma\sigma'} \simeq \Big(\frac{J_L J_R}{\epsilon_0}\Big)^2 \langle n| e^{-i\phi} |n'\rangle|^2 |\mathcal{R}_{\sigma'\sigma}|^2 \ , \tag{A2}$$

with the spin-dependent part of $\mathcal{T}$ given by

$$\mathcal{R} = \mathcal{S}_R^\dagger (A_0 + i\mathbf{B}_0 \cdot \boldsymbol{\sigma}) \mathcal{S}_L \ . \tag{A3}$$

One notes that

$$\mathrm{Tr}\{\mathcal{R}\mathcal{R}^\dagger\} = 2 \ , \tag{A4}$$

and

$$\mathrm{Tr}\{\mathcal{R}\sigma_z\mathcal{R}^\dagger\sigma_z\} = 2[(A_0^2 - B_0^2)\hat{\mathbf{n}}_L\cdot\hat{\mathbf{n}}_R + 2A_0\mathbf{B}_0\cdot\hat{\mathbf{n}}_L\times\hat{\mathbf{n}}_R + 2(\mathbf{B}_0\cdot\hat{\mathbf{n}}_L)(\mathbf{B}_0\cdot\hat{\mathbf{n}}_R)] \ , \quad \text{(A5)}$$

where we have used

$$\mathcal{S}_{L,R}\sigma_z\mathcal{S}_{L,R}^\dagger = \hat{\mathbf{n}}_{L,R}\cdot\boldsymbol{\sigma} \ . \quad \text{(A6)}$$

The matrix $\mathcal{R}$ can be written as

$$\mathcal{R} = C + i\mathbf{D}\cdot\boldsymbol{\sigma}, \quad \text{(A7)}$$

with $C^2 + D_x^2 + D_y^2 + D_z^2 = 1$. Therefore, the diagonal elements of the matrix $\mathcal{R}$ are two complex conjugate numbers, and so are also the off diagonal elements. This implies that the diagonal elements of $|\mathcal{R}_{\sigma'\sigma}|^2$ are equal to one another, and the off diagonal ones are also identical. To derive explicit expressions for them, we note that the matrix $\mathcal{R}$ has the property

$$\mathrm{Tr}\{C + i\mathbf{D}\cdot\boldsymbol{\sigma})\sigma_z(C - i\mathbf{D}\cdot\boldsymbol{\sigma})\sigma_z\} = 2(C^2 + D_z^2 - D_x^2 - D_y^2) \ . \quad \text{(A8)}$$

It follows that the diagonal matrix elements (in spin space) of the transmission are $\mathcal{T}_{nn',\sigma\sigma} \equiv \mathcal{T}_{nn',\mathrm{d}} \equiv C^2 + D_z^2$ and the off diagonal ones are $\mathcal{T}_{nn',\sigma\overline{\sigma}} \equiv \mathcal{T}_{nn',\mathrm{nd}} \equiv D_x^2 + D_y^2$, with

$$\mathcal{T}_{nn',\mathrm{d}} = \frac{1}{2}\Big(\frac{J_L J_R}{\epsilon_0}\Big)^2 |\langle n|e^{-i\phi}|n'\rangle|^2\Big[1 + \Big((A_0^2 - B_0^2)\hat{\mathbf{n}}_L\cdot\hat{\mathbf{n}}_R + 2A_0\mathbf{B}_0\cdot\hat{\mathbf{n}}_L\times\hat{\mathbf{n}}_R + 2(\mathbf{B}_0\cdot\hat{\mathbf{n}}_L)(\mathbf{B}_0\cdot\hat{\mathbf{n}}_R)\Big)\Big] \ ,$$
$$\mathcal{T}_{nn',\mathrm{nd}} = \frac{1}{2}\Big(\frac{J_L J_R}{\epsilon_0}\Big)^2 |\langle n|e^{-i\phi}|n'\rangle|^2\Big[1 - \Big((A_0^2 - B_0^2)\hat{\mathbf{n}}_L\cdot\hat{\mathbf{n}}_R + 2A_0\mathbf{B}_0\cdot\hat{\mathbf{n}}_L\times\hat{\mathbf{n}}_R + 2(\mathbf{B}_0\cdot\hat{\mathbf{n}}_L)(\mathbf{B}_0\cdot\hat{\mathbf{n}}_R)\Big)\Big] \ . \quad \text{(A9)}$$

Returning now to the transmission matrix $\mathcal{A}$, Eq. (17), we find that it can be factorized into a temperature and magnetic filed dependent factor, and a spin-dependent factor, so that it takes the form given in the main text, Eqs. (27), (28), and (29).

[1] V. Sazonova, Y. Yaish, H. Üstünel, D. Roundy, T. A. Arias, and P. L. McEuen, Nature **431**, 284 (2004).
[2] B. Lassagne, Y. Tarakanov, J. Kinaret, D. Garcia-Sanchez, and A. Bachtold, Science **325**, 1107 (2009).
[3] G. A. Steele, A. K. Hüttel, B. Witkamp, M. Poot, H. B. Meerwaldt, L. P. Kouwenhoven, and H. S. J. van der Zant, Science **325**, 1103 (2009).
[4] J. Chaste, M. Sledzinska, M. Zdrojek, J. Moser, and A. Bachtold, Appl. Phys. Lett. **99**, 213502 (2011).
[5] E. A. Laird, F. Pei, W. Tang, G. A. Steele, and L. P. Kouwenhoven, Nano Lett. **12**, 193 (2012).
[6] A. Eichler, J. Moser, M. I. Dykman, and A. Bachtold, arXiv:1311.6589.
[7] K. Uchida, J. Xiao, H. Adachi, J. Ohe, S. Takahashi, J. Ieda, T. Ota, Y. Kajiwara, H. Umezawa, H. Kawai, G. E. W. Bauer, S. Maekawa, and E. Saitoh, Nature Materials **9**, 894 (2010).
[8] J. Xiao, G. E. W. Bauer, K. Uchida, E. Saito, and S. Maekawa, Phys. Rev. B **81**, 214418 (2010); *ibid.* Phys. Rev. B **82**, 099904 (E) (2010).
[9] H. Adachi, J. Ohe, S. Takahashi, and S. Maekawa, Phys. Rev. B **83**, 094410 (2011).
[10] M. Schreier, A. Kamra, M. Weiler, J. Xiao, G. E. W. Bauer, R. Gross, and S. T. B. Goennenwein, Phys. Rev. B **88**, 094410 (2013).
[11] A. B. Cahaya, O. A. Tretiakov, and G. E. W. Bauer, arXiv:1311.6195.
[12] A. Hoffmann, IEEE Trans. Magnetics **49**, 5172 (2013).
[13] B. F. Miao, S. Y. Huang, D. Qu, and C. L. Chien, Phys. Rev. Lett. **111**, 066602 (2013).
[14] J. Flipse, F. K. Dejene, D. Wagenaar, G. E. W. Bauer, J. Ben Youssef, and J. van Wees, arXiv:1311.4772.
[15] A. Dankert and S. P. Dash, arXiv:1403.3528.
[16] E. I. Rashba, Fiz. Tverd. Tela (Leningrad) **2**, 1224 (1960) [Sov. Phys. Solid State **2**, 1109 (1960)]; Y. A. Bychkov and E. I. Rashba, J. Phys. C **17**, 6039 (1984).
[17] Note that the situation at hand is more complicated than a simple spin rotation. While moving along a particular spatial path, the electron spin rotates around an axis whose orientation is constantly changing.
[18] S. Nadj-Perge, S. M. Frolov, E. P. A. M. Bakkers, and L. P. Kouwenhoven, Nature **468**, 1084 (2010); X-J. Hao,T. Tu, G. Cao, C. Zhou, H-O. Li, G-C. Guo, W. Y. Fung, Z. Ji, G-P. Guo, and W. Lu, Nano Letts. **10**, 2956 (2010);
[19] F. Kuemmeth, S. Ilani, D. C. Ralph, and P. L. McEuen, Nature **452**, 448 (2008).
[20] R. I. Shekhter, O. Entin-Wohlman, and A. Aharony, Phys. Rev. Lett. **111**, 176602 (2013); see also Supplemental Material at http://link.aps.org/supplemental/10.1103/ PhysRevLett.111.176602.
[21] This means that the internal relaxation taking place within the electrodes is much faster as compared with the charge relaxation in the weak link. This very fact allows us to assume local equilibrium in each of the reservoirs.
[22] B. Göhler, V. Hamelbeck, T. Z. Markus, M. Kettner, G.

F. Hanne, Z. Vager, R. Naaman, and H. Zacharias, Science **331**, 894 (2011); D. Mishraa, T. Z. Markusa, R. Naaman, M. Kettnerb, B. Göhlerb, H. Zachariasb, N. Friedmanc, M. Shevesc, and C. Fontanesid, PNAS **110**, 14872 (2013).

[23] K. Koyama and H. Merz, Z. Physik B **20**, 131 (1975); M. Wöhlecke and G. Borstel, Physica Status Solidi (b) **106**, 593 (1981); C. J. Tabert and E. J. Nicol, Phys. Rev. Lett. **110**, 197402 (2013); C. Jozwiak, C-H. Park, K. Gotlieb, C. Hwang, D-H. Lee, S. G. Louie, J. D. Denlinger, C. R. Rotundu, R. J. Birgeneau, Z. Hussain, and A. Lanzara, Nature Physics **9**, 293 (2013).

[24] The case of nonmagnetic electrodes poses no problem, as the orientation of the spins there can always be chosen as that of the injected electrons.

[25] R. I. Shekhter, L. Y. Gorelik, L. I. Glazman, and M. Jonson, Phys. Rev. Lett. **97**, 156801 (2006).

[26] This is a widely-accepted picture, see e.g., M. J. Biercuk, S. Ilani, C. M. Marcus, and P. L. McEuen, in *Carbon nanotubes*, edited by A. Jorio, G. Dresselhaus, and M. S. Dresselhaus, Topics Applied Physics, Vol. **111** (Springer-Verlag, Berlin, Heidelberf, 2008).

[27] Y. Meir, Y. Gefen, and O. Entin-Wohlman, Phys. Rev. Lett. **63**, 798 (1989); Y. Oreg and O. Entin-Wohlman, Phys. Rev. B **46**, 2393 (1992); T. V. Shahbazyan and M. E. Raikh, Phys. Rev. Lett. **75**, 1408 (1994); O. Entin-Wohlman, A. Aharony, Y. M. Galperin, V. I. Kozub, and V. Vinokur, *ibid.* **95**, 086603 (2005).

[28] An alternative geometry, with $x_L = x_R = d/2$ and $y_L = y_R = (d/2)\tan(\theta)$, gives similar results.

[29] Note the peculiar way of defining the transmission as given in Eq. (14): it has dimensions of energy squared because it is not yet multiplied by the appropriate densities of states. The (dimensionless) transmission probabilities are given in Eqs. (20).

[30] It should be noted that had we included the electron-vibration interaction to higher orders, we would have obtained a tiny modification of the conductance due to the spin-orbit interaction.

Supplemental material

1. The expansion in terms of the boson operators

Our model aims to mimic the bending vibrations of the suspended nanowire. This is why once the mechanical bending of the wire by an angle θ_0 is achieved, the distance along x between the two supporting leads is fixed, while the red dot in Fig. 2 experiences a vibrational shift Δy along y. This vibrational motion mimics the bending vibration of the suspended nanowire around its equilibrium position $\theta = \theta_0$. Hence

$$\tan\theta = 2y/\ell \Rightarrow \Delta\theta/\cos^2(\theta_0) = 2\Delta y/\ell \ , \tag{A10}$$

where ℓ is the projection on the $x-$axis of the wire length d,

$$\ell = d\cos(\theta_0) \ . \tag{A11}$$

It follows that

$$\Delta\theta = \frac{2}{\ell}\cos^2(\theta_0)\Delta y = \frac{2\cos(\theta_0)}{d}\Delta y \ . \tag{A12}$$

The result is the main text is obtained upon expanding $\Delta y = (a_0/2)(b + b^\dagger)$ to linear order in the vibrational modes' operators.